The Astrophysical Journal, 616:L75–L78, 2004 December 1

EFFECT OF HOT BARYONS ON THE WEAK-LENSING SHEAR POWER SPECTRUM

Hu Zhan and Lloyd Knox
Department of Physics, University of California at Davis, 1 Shields Avenue, Davis, CA 95616;
zhan@physics.ucdavis.edu, lknox@physics.ucdavis.edu
Received 2004 September 8; accepted 2004 October 13; published 2004 October 25

ABSTRACT

We investigate the impact of the intracluster medium on the weak-lensing shear power spectrum (PS). Using a halo model we find that, compared to the dark matter–only case, baryonic pressure leads to a suppression of the shear PS on the order of a few percent or more for $l \gtrsim 1000$. Cooling/cooled baryons and the intergalactic medium can further alter the shear PS. Therefore, the interpretation of future precision weak-lensing data at high multipoles must take into account the effects of baryons.

Subject headings: cosmology: theory — dark matter — galaxies: clusters: general — gravitational lensing — large-scale structure of universe

1. INTRODUCTION

Weak gravitational lensing is a promising technique for precision cosmology. Its chief advantage over other techniques comes from its sensitivity to the total density field, rather than just the baryonic component. Since the total density is mostly due to the dark matter, which only interacts gravitationally, the statistical properties of the total density field can be calculated ab initio with much higher accuracy than can observables that are more directly dependent on baryons. Combined with the enormous statistical power of proposed survey projects, such as the Large Synoptic Survey Telescope[1] and *SuperNova/Acceleration Probe*,[2] weak lensing is thought to be capable of determining (some) cosmological parameters to a few percent level (e.g., Refregier et al. 2004).

Many studies of weak-lensing statistics assume baryons to trace dark matter exactly (e.g., Bacon et al. 2000; Cooray et al. 2000; Hu & White 2001; Song & Knox 2003). This allows one to predict the weak-lensing shear power spectrum (PS) from the nonlinear dark matter PS that is well calibrated using *N*-body simulations (Peacock & Dodds 1996; Ma & Fry 2000; Smith et al. 2003).

However, more than 10% of the total mass is in baryons, which do not follow dark matter exactly on small scales. Therefore, the total mass distribution and its PS will deviate somewhat from those in a universe that has the same initial conditions except that all the mass is in dark matter.[3] Such a deviation in the mass PS will result in a difference in weak-lensing statistics. Eventually, it will be necessary to account for the baryonic influence on the shear PS as we reach for the projected statistical power of weak-lensing surveys.

Baryons exist mainly in three categories: (1) cooling/cooled baryons such as in stars and galaxies, (2) hot baryons or the intracluster medium (ICM), and (3) the intergalactic medium (IGM). The cooling/cooled baryons alter the statistics of gravitational lensing (White 2004) because they can condense to a much denser state than dark matter, which in turn modifies the dark matter distribution (Kazantzidis et al. 2004). The ICM is smoother than cooling/cooled baryons, so that the effect might be much less pronounced (White 2004). However, the ICM greatly outweighs the baryons in the galaxies. Therefore, it could still have a significant impact on the shear PS. Indeed, we find that at $l \lesssim 3000$, the ICM has a larger impact on the shear PS than do the cooling/cooled baryons.

For completeness we note here that the IGM is much more diffuse than the other two, but it is the largest reservoir of baryons. Since the density fluctuations on the angular scales that we consider are dominated by high-density and massive objects, we neglect the IGM for the present but plan to study its effect using hydrodynamical simulations in the future.

In this Letter we demonstrate the effect of hot baryons on the weak-lensing shear PS. Assuming an isothermal β-model (Cavaliere & Fusco-Femiano 1976), we are able to extend the halo model (for a review, see Cooray & Sheth 2002) to include hot baryons in the total mass PS, which is then used to calculate the shear PS. Aside from the uncertainties of shear statistics due to halo parameters (Takada & Jain 2003), this method is not sufficiently accurate for interpreting future data because we have not included all the baryons and because we have made simple associations of the ICM profile with its dark matter halo. Nonetheless, it provides a framework for analytically estimating the effect of uncertainty in the clustering properties of hot baryons.

2. MASS POWER SPECTRUM

Realistic halo profiles (e.g., Navarro et al. 1996; Moore et al. 1999) enable the halo model to reproduce the nonlinear dark matter PS. With the one-halo PS $P_{\rm dm}^{\rm 1h}(k)$ and two-halo PS $P_{\rm dm}^{\rm 2h}(k)$, the dark matter PS $P_{\rm dm}(k)$ can be approximated by (Peacock & Smith 2000; Ma & Fry 2000; Seljak 2000; Scoccimarro et al. 2001)

$$\begin{aligned} P_{\rm dm}(k) &= P_{\rm dm}^{\rm 1h}(k) + P_{\rm dm}^{\rm 2h}(k), \\ P_{\rm dm}^{\rm 1h}(k) &= \int f(\nu) d\nu\, m_d(\nu) |u_d[k, m_d(\nu)]|^2 / \bar{\rho}_d, \\ P_{\rm dm}^{\rm 2h}(k) &= P_L(k) \left\{ \int f(\nu) b(\nu) d\nu\, u_d[k, m_d(\nu)] \right\}^2, \end{aligned} \tag{1}$$

where $\bar{\rho}_d$ is the mean density of the universe at the present, $u_d[k, m_d(\nu)]$ is the normalized profile of a dark matter halo with mass m_d in Fourier space (e.g., Cooray & Sheth 2002), and P_L is the linear mass PS. The dark matter density profile is cut

[1] See http://www.lsst.org.
[2] See http://snap.lbl.gov.
[3] One may think of this as an *N*-body simulation of dark matter that has the same parameters and initial mass PS (including baryonic features such as due to acoustic oscillations) as a full hydrodynamical simulation.

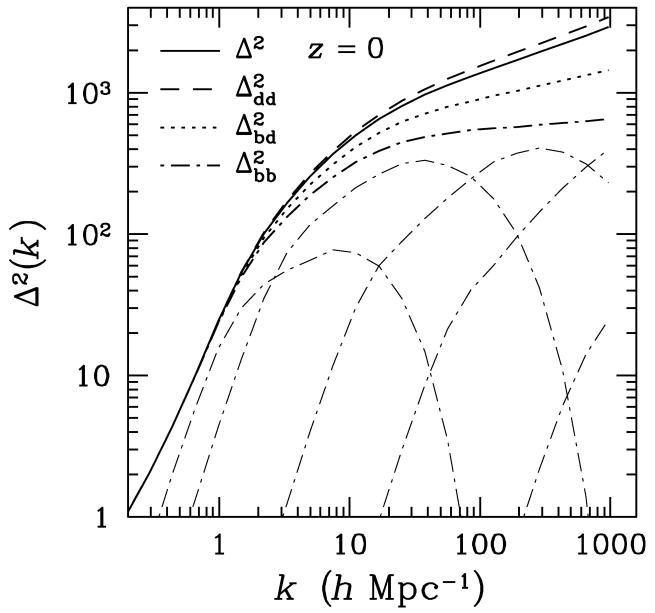

FIG. 1.—Halo-model mass PS at $z = 0$. The total PS $\Delta^2(k)$ (*solid line*) is calculated using eq. (3) as a weighted sum of the dark matter PS $\Delta^2_{dd}(k)$ (*dashed line*), the baryon–dark matter cross PS $\Delta^2_{bd}(k)$ (*dotted line*), and the baryon PS $\Delta^2_{bb}(k)$ (*dash-dotted line*). From left to right, the thin dash-dotted lines represent one-halo contributions to the baryon PS from mass ranges of $10^{17}\ M_\odot \geq m_d > 10^{14}\ M_\odot$, $10^{14}\ M_\odot \geq m_d > 10^{12}\ M_\odot$, $10^{12}\ M_\odot \geq m_d > 10^{10}\ M_\odot$, $10^{10}\ M_\odot \geq m_d > 10^{7}\ M_\odot$, and $10^{7}\ M_\odot \geq m_d \geq 10^{4}\ M_\odot$.

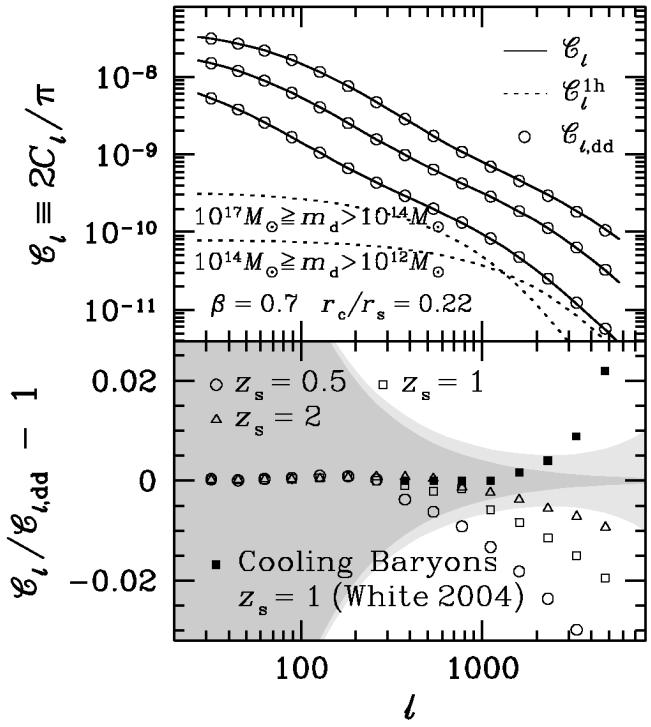

FIG. 2.—*Upper panel*: Shear PS with and without baryons (*solid lines and open circles, respectively*). From bottom to top, the solid lines and open circles assume sources to be on a thin slice at $z = 0.5$, 1, and 2. The dotted lines represent one-halo contributions to the total shear PS C_l at $z = 0.5$. Contributions from halos with mass less than $10^{12}\ M_\odot$ are below 10^{-12}. The fractional difference is shown in the lower panel. The dark gray band is the 1 σ statistical error on a band of width $l/4$ in the sample variance limit for a survey with $f_{sky} = 0.25$. The light gray band includes shape noise for the $z_s = 1$ PS assuming $\bar{n} = 10$ arcmin^{-2} and $\gamma_{rms} = 0.2$.

off at the virial radius. The height of the density peak, ν, is defined as

$$\nu = [\delta_c(z)/\sigma(m_d)]^2, \quad (2)$$

where $\delta_c(z) \simeq 1.686\Omega_m^{0.0055}(z)$ (Hiotelis 2003) is the overdensity

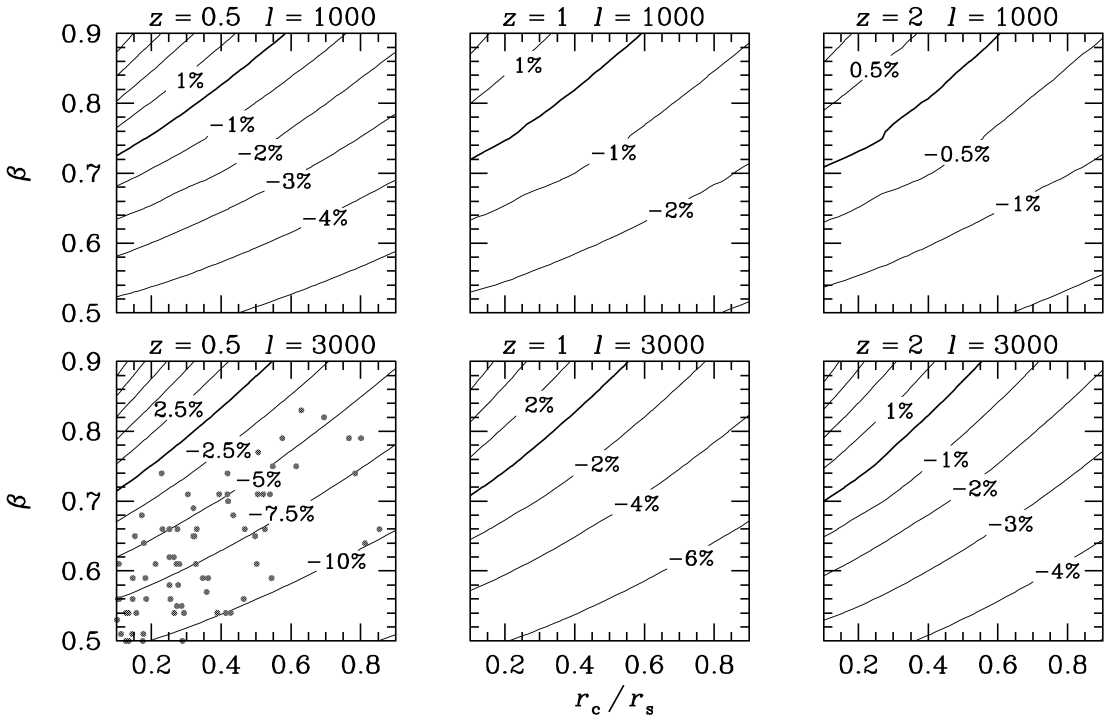

FIG. 3.—Contours of the fractional difference, $C_l/C_{l,dd} - 1$, in (β, r_c/r_s)-space. The gray dots in the lower left panel correspond to the observed values of β and r_c/r_s from MME99 and OM04.

of a spherical region that collapses at redshift z, $\Omega_m(z)$ is the ratio of matter density to critical density at z, and $\sigma(m_d)$ is the rms value of the density contrast $\delta\rho_d/\rho_d$ within a radius of $(3m_d/4\pi\bar{\rho}_d)^{1/3}$ at z. Equation (2) also defines $m_d(\nu)$. The functions $f(\nu)$ and $b(\nu)$, related to the halo mass function and bias, respectively, have the forms (Sheth & Tormen 1999)

$$\nu f(\nu) = A(1 + \nu_1^{-p})\nu_1^{1/2}e^{-\nu_1/2},$$
$$b(\nu) = 1 + (\nu_1 - 1)\delta_c^{-1} + 2p\delta_c^{-1}(1 + \nu_1^p)^{-1},$$

with $\nu_1 = 0.707\nu$ and $p = 0.3$. The normalization constant A satisfies the constraint $\int f(\nu)d\nu = 1$.

Equation (1) can be extended to include hot baryons:

$$P(k) = \sum_{ij} f_i f_j P_{ij}(k),$$
$$P_{ij} = P_{ij}^{1h} + P_{ij}^{2h},$$
$$P_{ij}^{1h} = \int f(\nu)d\nu\, m_d(\nu)u_i[k, m_d(\nu)]u_j[k, m_d(\nu)]/\bar{\rho}_d,$$
$$P_{ij}^{2h} = P_L(k)\int f(\nu)b(\nu)d\nu\, u_i[k, m_d(\nu)] \times \int f(\nu')b(\nu')d\nu'\, u_j[k, m_d(\nu')], \quad (3)$$

where the subscripts $i, j = d$ for dark matter and b for baryons. The coefficients, f_d and f_b, are the fractions of dark matter and baryons in total halo mass, respectively. Obviously, $P_{ij}(k) = P_{ji}(k)$, $f_d + f_b = 1$, and equation (1) is a special case of equation (3) when $f_b = 0$.

For equation (3) we have assumed a fixed gas-mass fraction f_b. In principle, there is a distribution of f_b for a given halo mass, and this distribution can be dependent on halo mass (or on the ICM temperature; see Arnaud & Evrard 1999 and Mohr et al. 1999, hereafter MME99). Although the dependence is found to be weak for clusters (Ota & Mitsuda 2004, hereafter OM04), it may not be true for low-mass systems. Hence, an average over the distribution should be incorporated to calculate the PS. We assume for convenience that f_b equals the cosmic mean baryon fraction of 0.13.

The Fourier-space baryon profile $u_b(k, m_d)$ is calculated from the β-model, $\rho_b(r) = \rho_{b0}(1 + r^2/r_c^2)^{-3\beta/2}$, where $\rho_{b,0}$ is the central baryon density, r_c is the core radius, and $\beta = 0.4$–1.2 (MME99; OM04; Mulchaey et al. 2003; Ettori et al. 2004). The baryon profile is also cut off at the virial radius. Assuming hydrostatic equilibrium and the Navarro-Frank-White (NFW) halo profile (Navarro et al. 1996), Makino et al. (1998) find that the best-fitting β-model has a core radius about one-fifth of the scale radius, r_s, of the NFW profile. We choose $\beta = 0.7$ and $r_c = 0.22r_s$ to be the fiducial model and allow the parameters to vary. Note that the polytropic gas profile (Komatsu & Seljak 2001) is slightly smoother than our fiducial model and that it gives similar results.

Figure 1 shows the fiducial model PS at $z = 0$ in dimensionless form; i.e., $\Delta^2(k) = k^3P(k)/2\pi^2$. We have assumed a flat universe with $\Omega_m = 0.3$, $\Gamma = 0.18$, $\sigma_8 = 0.85$, and $n = 1$, where Γ is the shape parameter of the PS, σ_8 is the rms value of the density contrast within a radius of 8 h^{-1} Mpc, and n is the power spectral index. Because, for the fiducial model, the baryon profile is smoother than the dark matter profile, the baryon PS $\Delta^2_{bb}(k)$ and baryon–dark matter cross PS $\Delta^2_{bd}(k)$ become significantly lower than the dark matter PS $\Delta^2_{dd}(k)$ on small scales ($k > 1$ h Mpc^{-1}) where the one-halo term dominates. At higher redshift, this departure occurs at a larger wavenumber. Consequently, the total mass PS is lower than what it would be if the hot baryons were replaced by dark matter.

From the breakdown of one-halo contributions to the baryon PS, also shown in Figure 1, one sees that each group of halos dominates a certain range of scales. The β-model might not apply to halos with $m_d < 10^{10}$ $M_\odot$, but since they contribute little to the mass PS at $k < 100$ h Mpc^{-1}—the most important scales to shear PS at l less than a few thousand—our conclusions will not be affected.

3. SHEAR POWER SPECTRUM

With the Limber approximation and the assumption that sources are on a thin slice at z, the shear PS C_l in a flat universe is given by (Bacon et al. 2000; Hu 2000; Bartelmann & Schneider 2001)

$$C_l = \frac{9}{4}\left(\frac{H_0}{c}\right)^4\left(\frac{\Omega_m}{D_s}\right)^2\int_0^{D_s} dD\left(\frac{D_s - D}{a}\right)^2 P(k;\ z), \quad (4)$$

where H_0 is the Hubble constant at $z = 0$, c is the speed of light, D and D_s are the comoving distance of the lens and sources, respectively, $a = (1 + z)^{-1}$, and $k = l/D$. We define $\mathcal{C}_l \equiv 2C_l/\pi$, which is the contribution to the variance of the deflection angle from logarithmic intervals in l. The results are shown in Figure 2 for the fiducial model. Since the shear PS is mostly affected by the linear and quasi-linear part of the mass PS, the effect of hot baryons on the shear PS is less than a few percent for $l \lesssim 3000$. As redshift increases, the same l corresponds to smaller wavenumbers, meanwhile the PS is more linear at the same wavenumber. In addition, hot baryons make less of a difference in the mass PS at higher redshift. Thus, the effect of the ICM on the shear PS reduces with increasing redshift.

The effect of the ICM on the shear PS is large enough that it will need to be addressed if the cosmological parameter errors forecasted in, e.g., Song & Knox (2003), with $l_{max} = 1000$, Hu (2002), with $l_{max} = 3000$, and Refregier et al. (2004), with $l_{max} = 2 \times 10^5$, are to be realized. This is clear from the lower panel of Figure 2, where departures outside the shaded region are larger than the statistical error for a fiducial survey with parameter values as given in the caption. The statistical error in $\mathcal{C}_l$ in a band of width $l/4$ is given by

$$\Delta\mathcal{C}_l = 0.004\frac{1000}{l}\left(\frac{0.25}{f_{sky}}\right)^{1/2}\left(\mathcal{C}_l + \frac{2}{\pi}\frac{\gamma^2_{rms}}{\bar{n}}\right), \quad (5)$$

where f_{sky} is the fraction of sky covered, $\bar{n}$ is the surface number density of sources with measurable shapes, and γ^2_{rms} is the variance of the "shape noise."

From the breakdown of the contributions from different mass halos, one sees that the two-halo term in the mass PS is the largest contributor at large angular scales, and only those halos with $m_d > 10^{12}$ $M_\odot$ are important to the shear PS at l around a few thousand.

Observationally, the β-parameter and the core radius assume a range of values. In fact, the baryon profile becomes more compact than the dark matter profile if β is larger and if the core-radius–to–scale-radius ratio is smaller. This can drive the baryon–dark matter cross PS and baryon PS higher than the dark matter PS, and results in an increase in the shear PS. On

the other hand, the entropy floor (Ponman et al. 1999) can increase the core radius of the baryon profile in low-mass systems (Tozzi & Norman 2001; Holder & Carlstrom 2001) and reduce the total mass PS and shear PS.

Figure 3 explores the relative changes in the shear PS in the (β, r_c/r_s)-space for $l = 1000$ and 3000. We see that given the observational uncertainties about the β-model parameters, hot baryons could pose a significant challenge to precision cosmology.

We are optimistic that the challenge can be met, at least for $l \lesssim 3000$, by a combination of hydrodynamical simulations (which in principle can track hot baryons quite accurately) and observations of hot gas via X-ray emission and the Sunyaev-Zel'dovich (SZ) effect. Fortunately, it is only very massive halos that are important at $l \lesssim 3000$, and these are just the easiest ones to study in X-ray emission and the SZ effect. Planned SZ surveys such as the South Pole Telescope, Atacama Cosmology Telescope, Atacama Pathfinder Experiment, and Sunyaev-Zel'dovich Array will have sufficient angular resolution and observe a sufficiently large number of clusters to guide the development of a statistical model of ICM profiles. An observing strategy can also, to some degree, mitigate the difficulties posed by baryons. Their importance at small scales argues for large sky coverage, to reduce sample variance (thereby improving the C_l measurement on all scales), rather than depth and angular resolution, which reduce the shape noise that is only important at small scales.

4. DISCUSSION AND CONCLUSIONS

We have extended the halo model to calculate the total mass PS of dark matter and hot baryons. Given the observed properties of the ICM, we find that the total mass PS is considerably lower than the dark matter PS on small scales. This leads to a few percent reduction of the shear PS at $1000 \lesssim l \lesssim 3000$ compared to what it would be if baryons traced dark matter exactly. The effect grows with increasing l. Furthermore, for $l \gtrsim 3000$ an effect (with opposite sign; see Fig. 2) also becomes important as a result of cooling/cooled baryons (White 2004).

So far, we have not considered the IGM (including the warm-hot IGM; Davé et al.2001), which contains roughly two-thirds of the baryons at $z = 0$. Using hydrodynamical simulations (TreeSPH; Davé et al. 1997) that incorporate cooling, heating, star formation, and feedback, Zhan (2004) obtains a total baryon PS that is lower than what has been shown in Figure 1. Therefore, when all the baryons are accounted for, the effect on weak-lensing statistics could be even greater. A detailed investigation using hydrodynamical simulations will be necessary to assess the total baryon effect. In conclusion, for precision cosmology with weak lensing to live up to its promise, we will have to pay attention to the modeling of baryons and not just the dark matter.

We thank C. Fassnacht, L. Lubin, A. Stebbins, J. A. Tyson, and M. White for useful discussions. This work was supported by the NSF under grant 0307961 and by NASA under grant NAG5-11098.

REFERENCES

Arnaud, M., & Evrard, A. E. 1999, MNRAS, 305, 631
Bacon, D. J., Refregier, A. R., & Ellis, R. S. 2000, MNRAS, 318, 625
Bartelmann, M., & Schneider, P. 2001, Phys. Rep., 340, 291
Cavaliere, A., & Fusco-Femiano, R. 1976, A&A, 49, 137
Cooray, A., Hu, W., & Miralda-Escudé, J. 2000, ApJ, 535, L9
Cooray, A., & Sheth, R. 2002, Phys. Rep., 372, 1
Davé, R., et al. 2001, ApJ, 552, 473
Davé, R., Dubinski, J., & Hernquist, L. 1997, NewA, 2, 277
Ettori, S., Tozzi, P., Borgani, S., & Rosati, P. 2004, A&A, 417, 13
Hiotelis, N. 2003, MNRAS, 344, 149
Holder, G. P., & Carlstrom, J. E. 2001, ApJ, 558, 515
Hu, W. 2000, Phys. Rev. D, 62, 043007
———. 2002, Phys. Rev. D, 65, 023003
Hu, W., & White, M. 2001, ApJ, 554, 67
Kazantzidis, S., Kravtsov, A. V., Zentner, A. R., Allgood, B., Nagai, D., & Moore, B. 2004, ApJ, 611, L73
Komatsu, E., & Seljak, U. 2001, MNRAS, 327, 1353
Ma, C.-P., & Fry, J. N. 2000, ApJ, 543, 503
Makino, N., Sasaki, S., & Suto, Y. 1998, ApJ, 497, 555
Mohr, J. J., Mathiesen, B., & Evrard, A. E. 1999, ApJ, 517, 627 (MME99)
Moore, B., Quinn, T., Governato, F., Stadel, J., & Lake, G. 1999, MNRAS, 310, 1147
Mulchaey, J. S., Davis, D. S., Mushotzky, R. F., & Burstein, D. 2003, ApJS, 145, 39
Navarro, J. F., Frenk, C. S., & White, S. D. M. 1996, ApJ, 462, 563
Ota, N., & Mitsuda, K. 2004, A&A, in press (astro-ph/0407602) (OM04)
Peacock, J. A., & Dodds, S. J. 1996, MNRAS, 280, L19
Peacock, J. A., & Smith, R. E. 2000, MNRAS, 318, 1144
Ponman, T. J., Cannon, D. B., & Navarro, J. F. 1999, Nature, 397, 135
Refregier, A., et al. 2004, AJ, 127, 3102
Scoccimarro, R., Sheth R. K., Hui, L., & Jain, B. 2001, ApJ, 546, 20
Seljak, U. 2000, MNRAS, 318, 203
Sheth, R. K., & Tormen, G. 1999, MNRAS, 308, 119
Smith, R. E., et al. 2003, MNRAS, 341, 1311
Song, Y.-S., & Knox, L. 2003, Phys. Rev. D, 68, 043518
Takada, M., & Jain, B. 2003, MNRAS, 344, 857
Tozzi, P., & Norman, C. 2001, ApJ, 546, 63
White, M. 2004, Astropart. Phys., in press (astro-ph/0405593)
Zhan, H. 2004, Ph.D. thesis, Univ. Arizona (astro-ph/0408379)